Proceedings World Geothermal Congress 2020+1
Reykjavik, Iceland, April - October 2021

Numerical Simulation of Heat Extraction of CO_2-EGS with THM Coupling Method Based on Discrete Fracture Models

SUN Zhixue[a], JIANG Chuanyin[a], ZHANG Kai[a], MAO Qiangqiang[a], Kelvin BONGOLE[a] and XIN Ying[a]

[a] College of Petroleum Engineering, China University of Petroleum (East China), Qingdao, China, 266580

E-mails: upcszx@upc.edu.cn (SUN Zhixue); chuanyin_jiang@foxmail.com (JIANG Chuanyin); reservoirs@163.com (Zhang Kai); upcmaoqiangqiang@outlook.com (MAO Qiangqiang); kbongole@yahoo.com (Kelvin BONGOLE); 15764220169@163.com (XIN Ying)

Keywords: Heat extraction, CO_2-EGS, Discrete fracture network, THM coupled processes

ABSTRACT

The enhanced geothermal system (EGS) becomes the key technology of extracting heat from Hot Dry Rock (HDR) as it constructs an artificial thermal reservoir by hydraulic fracturing. Furthermore, geothermal development using carbon dioxide as the work fluid can achieve the CO_2 geological sequestration and concurrently bring additional benefits. In this paper, using the local thermal non-equilibrium theory, a numerical approach is presented to simulate the thermal-hydraulic-mechanical (THM) coupling processes and heat production performance of CO_2-EGS. The reservoir models consist of impermeable matrix and synthetic fracture networks with a power-law length distribution. A sequence of fracture network topologies and three different injection pressures are considered to investigate the influences of the geometrical distribution and hydraulic regimes. By analyzing the evolutions of equivalent permeability and heat production, the fracture network with a high connectivity still performs a wide thermal sweep under the high pressure gradient but that with a low connectivity gains a rapid decline in heat extraction efficiency with the pressure gradient increasing. The results show the geometrical and hydraulic effects play critical roles in the heat extraction efficiency and service life. In addition, the observation of two interactively superimposed processes has important implications for estimating the effectiveness of hydraulic fracturing in CO_2-EGS.

1. INTRODUCTION

With liquid-like density and gas-like viscosity, the supercritical CO_2 could be a superior work fluid for EGS and CO_2-EGS can especially achieve CO_2 geological sequestration as an ancillary benefit (Pruess, 2006). However, heat extraction of EGS involves complex multi-physical field interactions including heat transfer, fluid seepage and solid deformation which makes numerical method recognized as a viable approach to analyze the coupling processes (Mcdermott et al., 2006). In recent years, many useful models have been developed for modeling the performance of EGS (Xu et al., 2015; Zhao et al., 2015; Izadi and Elsworth, 2015). The previous work has proposed a THM coupling method based on the discrete fracture network (DFN), which shows high efficiency and astringency for dense fracture networks (Sun et al., 2017). However, little effort has been devoted to considering the complexity of fracture network topology. Otherwise, the superimposed influence of hydraulic regimes is critical to the heat transfer of fracture rocks (Gisladottir et al., 2016). Thus, this paper aims to investigate how these two aspects interactively affect the THM coupling processes of CO_2-EGS. Our results have important implications for many engineering applications such as estimating the effectiveness of hydraulic fracturing.

2. METHODOLOGY

2.1 Discrete fracture network modelling

The fracture distributions follow a power-law model which can describe the length distribution of fractures as (Bonnet et al., 2001):

$$n(l,L) = \alpha L^D l^{-a}, \text{ for } l \in [l_{\min}, l_{\max}] \tag{1}$$

Where, l, L, a, D, α, $l_{\min}$, $l_{\max}$ are fracture length, elementary volume of characteristic scale, fracture length characteristic exponent, fractal dimension and fracture density constant, the smallest length and largest fracture length, respectively. The smaller exponent a means the greater proportion of large fractures with respect to the smaller ones. The fracture intensity I and percolation parameter P of fracture networks are calculated, respectively, as:

$$I = \frac{1}{L^2}\int_{A_L} n(l,L) l' \, dl \tag{2}$$

$$P = \frac{1}{L^2}\int_{A_L} n(l,L) l'^2 \, dl \tag{3}$$

where l' denotes the fracture length included in the domain of an area $A_L = L^2$. The higher P represents the more connected system. The network is statistically connected if P is greater than the percolation threshold P_c, which has a scale-invariant value of ~5.8 (Bour et al., 1997).

2.2 THM coupling mathematical model

Compared with water, CO_2 properties is more sensitive to pressure and temperature. The density and viscosity of CO_2 can be calculated based on CMG Winprop (Li et al., 2019) and the heat capacity generally depends on the empirical correlation to temperature (Cui et al., 2016). Since the reservoir pressure is extremely high (i.e. 77.42 - 77.91 MPa), CO_2 is assumed to remain liquid.

The validation of numerical model and other basic assumptions can be referred to our previous work [Sun et al., 2017]. The mass conservation equations, energy balance equation in the rock matrix and fractures can be given as follows:

In the rock matrix:

$$S\frac{\partial p}{\partial t}+\nabla\cdot(-\frac{\kappa_m}{\mu}\nabla p)=Q \tag{4}$$

$$C_m\rho_m\frac{\partial T_m}{\partial t}=\lambda_m\nabla^2 T_m \tag{5}$$

$$\frac{E}{2(1+v)}u_{i,jj}+\frac{E}{2(1+v)(1-2v)}u_{j,ji}-\alpha_B p_{,i}-\alpha_T\frac{E}{(1-2v)}T_{m,i}+F_i=0 \tag{6}$$

In the fractures:

$$d_f S\frac{\partial p}{\partial t}+\nabla\cdot(-\frac{\kappa_f}{\mu}\nabla p)=d_f Q \tag{7}$$

$$d_f\rho_f C_f\frac{\partial T_f}{\partial t}+d_f\rho_f\upsilon_f C_f\nabla T_f=d_f\nabla\cdot(\lambda_f\nabla T_f)+h\cdot(T_s-T_f) \tag{8}$$

$$u_n=\sigma'_n/k_n, u_s=\sigma'_s/k_s \tag{9}$$

Where, S, p, t, μ, Q, d_f, h, E, v, u_i, α_B, α_T, $T_{m,i}$, F_i are specific storage, pressure, time, fluid dynamic viscosity, source term, fracture aperture, convection coefficient, elastic modulus, Poisson's ratio, displacement, Biot's constants, thermal expansion coefficient, temperature increment and body force per unit volume in the i-coordinate ($i = x, y$ in 2D), respectively. C, κ, ρ, λ, T, υ are heat capacity, permeability, density, thermal conductivity, temperature and volumetric flow flux. The subscripts "m" and "f" mean the matrix and fluid in the fractures respectively. u, σ' and k denote displacement, effective stress and stiffness. The subscripts ''n" and ''s" represent normal and tangential directions to the fracture plane respectively.

The hydraulic-mechanical (HM) coupling effect are dependent on the evolution of fracture permeability, which can be expressed as the following equation (10) (Miller 2016). When the effective normal stress is positive, the compressive stress induces fracture closure and permeability decreasing, otherwise the tensile stress means fracture opening and permeability increasing.

$$\kappa_f=\kappa_0 e^{-\alpha\sigma'_n}, \kappa_0=d_f^2/12 \tag{10}$$

3. RESULTS AND DISCUSSIONS

3.1 Numerical model set-up

The discrete fracture networks are constructed in a squared domain of size L = 10 m where the bounds of fracture length are given by $l_{min} = L/50 = 0.2$ m and $l_{max} = 50L = 500$ m and the location and orientation of fractures are assumed purely random (i.e. $D = 2.0$). As Figure 1 shows, we explore five different length exponent cases, i.e. a = 1.5, 2.0, 2.5, 3.0 and 3.5, and two different mean fracture intensity scenarios, i.e. I = 2.5 and 5.0 m^{-1}. Otherwise, ten realizations for each combination of a and I are generated.

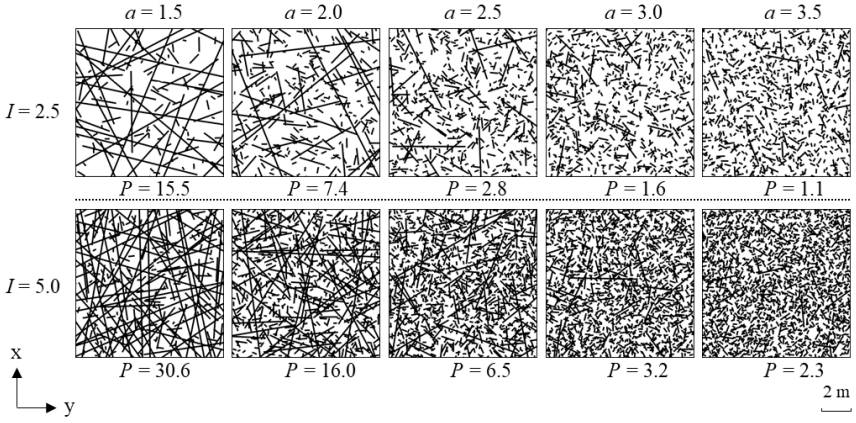

Figure 1 The exhibition of the generated synthetic DFN models

Considering the extremely low porosity and permeability in the matrix, the effect of the formation elasticity can be neglected, i.e. S = 0. Table 1 shows the other computational parameters used in this study. Initial and boundary conditions are as follows:

a) In seepage field, the given pressures are set on the left boundary (assumed as injection well) and right boundary (production well). The outlet pressure is invariable, i.e. 75.00 MPa and three different inlet pressures (i.e. 75.01 MPa, 75.10 MPa, 76.00 MPa) are applied to study the effect of the hydraulic regimes. The other external boundaries are impermeable.

b) In thermal field, the temperature of fractures and matrix at injection well is 20℃ and the initial reservoir temperature is 200℃. The top and bottom boundaries are adiabatic.

c) In displacement field, for focusing on the effects of pressurized CO_2 injection and heat extraction on the stress field, the initial geo-stress in the reservoir is not taken into account. Therefore, all the external boundaries are set as fixed constraint.

Table 1 Parameters of THM coupling analysis

λ_f (W/m/K)	ρ_s (kg/m^3)	C_m (J/kg/K)	λ_m (W/m/K)	κ_m (m^2)	d_f (mm)	α_T (K^{-1})	α (Pa^{-1})
0	2700	1000	3	1.0×10^{-18}	0.05	2.0×10^{-6}	0.2×10^{-6}
α_B	E (GPa)	v	k_s (GPa/m)	k_n (GPa/m)	h (W/m^2/K)		
1	30	0.25	400	1200	3000		

3.2 Results and analysis

Figure 2 exhibits the rock temperature distributions with different fracture network topology at $t = 3\times10^5$ s. when the fracture networks are disconnected, the temperature variation entirely depends on the heat conduction of matrix in which case the velocity of cold front propagation keeps constant with the fracture topology and pressure gradient. When the fracture networks are connected, the heat advection between fracture and matrix accelerates the heat transfer and the increasing injection pressure moves the cold front faster. Furthermore, the fracture networks with high connectivity or large percolation P have the reduced average matrix block size which improves heat exchange and increase heat sweep efficiency of the system.

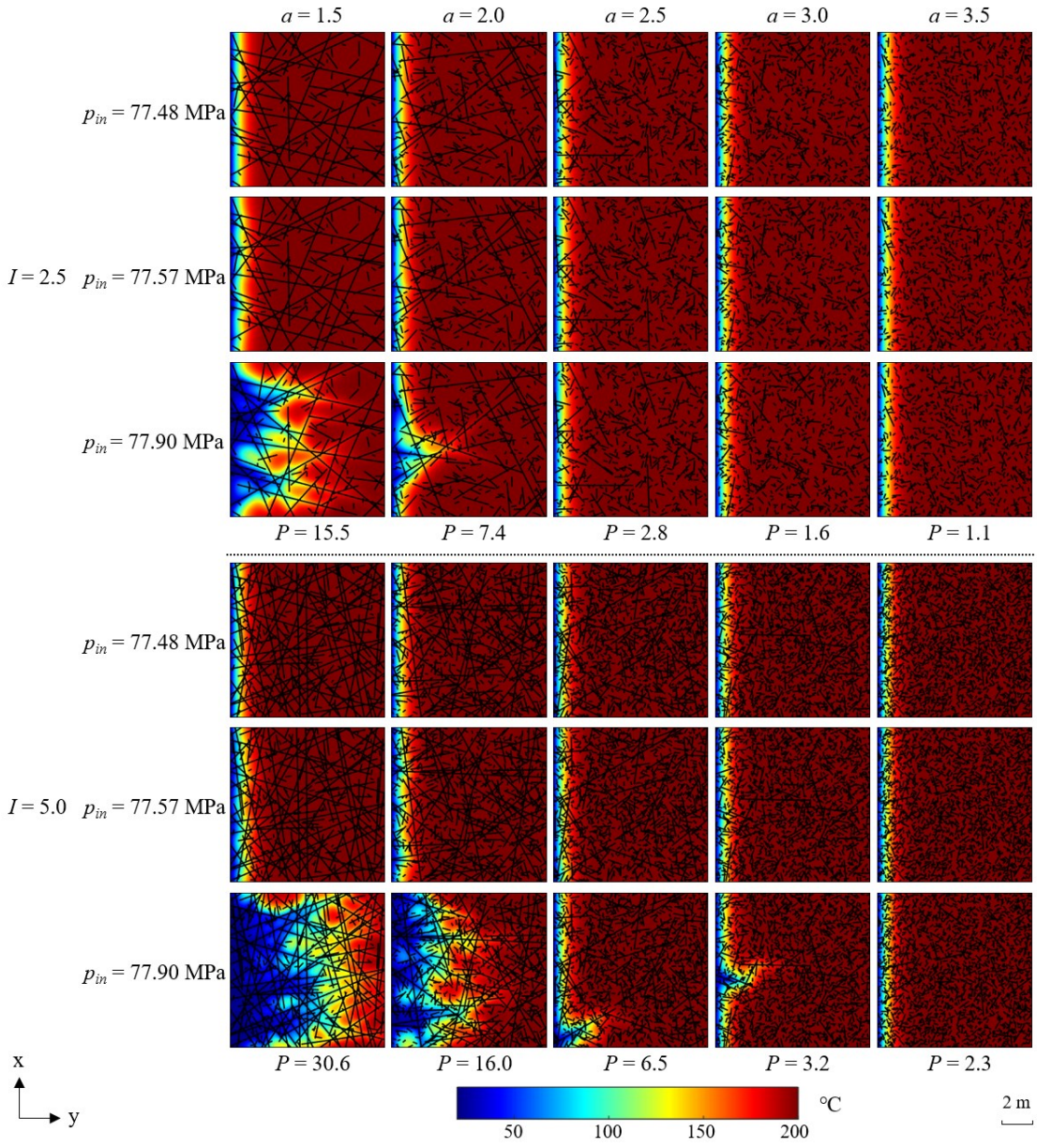

Figure 2 The rock temperature distributions with different fracture network topology ($t = 3 \times 10^5$ s)

Figure 3 shows the evolutions of the rock effective permeability with different fracture network and injection pressure. The stress distribution dependent on the injection pressurization and thermal expansion determines the permeability of fractures. With the cold fluid injection, the rock shrinkage enhances the permeability until the system heat is exhausted. The increasing injection pressure

expedites reaching the steady state but has little effect on the peak value, which indicates the influence of injection pressure variation on fracture permeability can be ignored in this study. Figure 4 gives the variation of the equivalent permeability as a function of the percolation parameter P at the initial and end time. An abrupt increase in permeability occurs once the fracture network becomes connected ($P > P_c$) and growth of the final permeability relative to the initial value depends on the thermal expansion coefficient α_T.

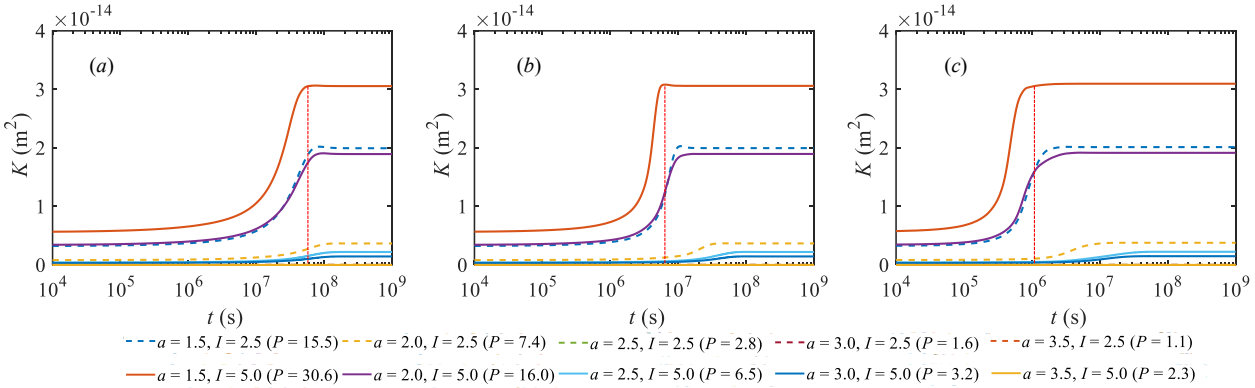

Figure 3 the evolutions of the rock effective permeability. (*a*) p_{in} = 75.01 MPa; (*b*) p_{in} = 75.10 MPa; (*c*) p_{in} = 76.00 MPa.

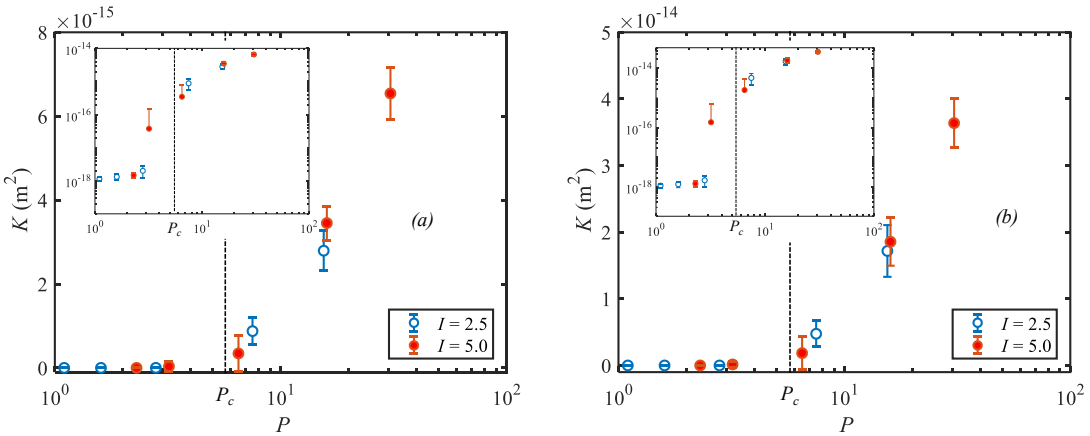

Figure 4 the variation of the equivalent permeability as a function of the percolation parameter *P* at (*a*) the initial time and (*b*) the end.

The average outlet temperature and overall heat recovery are the key parameters for evaluating the EGS running performance. The calculation equations can be given as follows (Nordqvist et al., 1992; Jiang et al., 2013; Yao et al., 2018):

$$T = \frac{\sum u_f d_f T_f + \int u_m T_m dy}{\sum u_f d_f + \int u_m dy} \tag{11}$$

$$\gamma = \frac{\iint_S [T_0 - T_m(t)] dV}{\iint_S (T_0 - T_{inj}) dV} \tag{12}$$

Where T, γ, T_0, T_{inj}, $T_m(t)$ are the average temperature, overall heat recovery, initial rock temperature, injection CO_2 temperature and rock matrix temperature at time t, respectively. Figure 5 and Figure 6 illustrate the evolutions of the two parameters. A stable running condition at the initial stage of development can be observed for all fracture networks. With the heat recovery further increasing, the low-temperature zone expands gradually to the production well and the heat production of the system decreases. The initial permeability (or percolation parameter) has a significant contribution to heat production in the critical period of geothermal development, i.e. the production temperature declining by 10% (Baria et al., 1999).

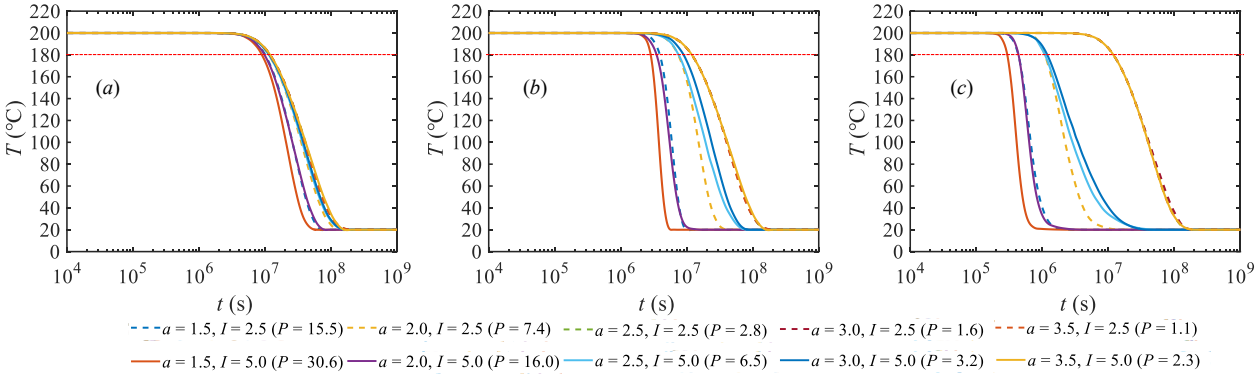

Figure 5 the evolutions of the average outlet temperature. (*a*) p_{in} = 75.01 MPa; (*b*) p_{in} = 75.10 MPa; (*c*) p_{in} = 76.00 MPa.

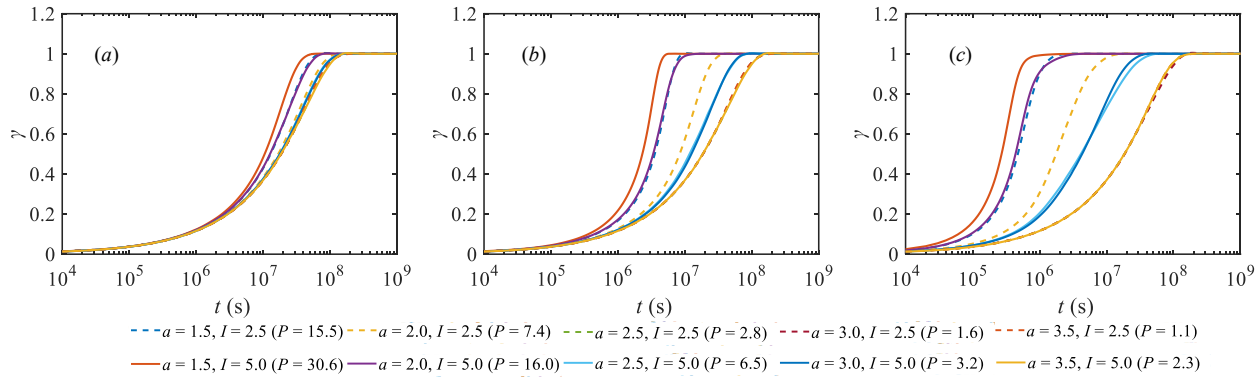

Figure 6 the evolutions of the overall heat recovery. (*a*) p_{in} = 75.01 MPa; (*b*) p_{in} = 75.10 MPa; (*c*) p_{in} = 76.00 MPa.

For better understanding the effect of the geometrical distribution and hydraulic regimes on heat extraction efficiency, the evolutions of $T \sim \gamma$ for the models are plotted in Figure 7. After the heat extraction is initiated, the average outlet temperature T evolves from 200 to 20 as γ varies from 0 to 1. At a specific T (e.g. T = 180 ℃), the higher corresponding γ means the more heat extracted during the period between 200 and T. For the disconnected reservoir, $\gamma_{(T = 180℃)}$ remains invariable at about 0.4 under different pressure gradient. For the fracture networks with a large percolation (e.g. P = 15.5), $\gamma_{(T = 180℃)}$ improves and subsequently declines with the growing injection pressure. However, the value can still reach up to about 0.56 at p_{in} = 76.00 MPa. For the fracture networks with a small percolation (e.g. P = 6.5 and 3.2), the contact area between injection liquid and rock is the smallest. In this condition, $\gamma_{(T = 180℃)}$ begins to decrease at p_{in} = 75.10 MPa and further drops to 0.21 at p_{in} = 76.00 MPa, which means more of heat is extracted at a low outlet temperature.

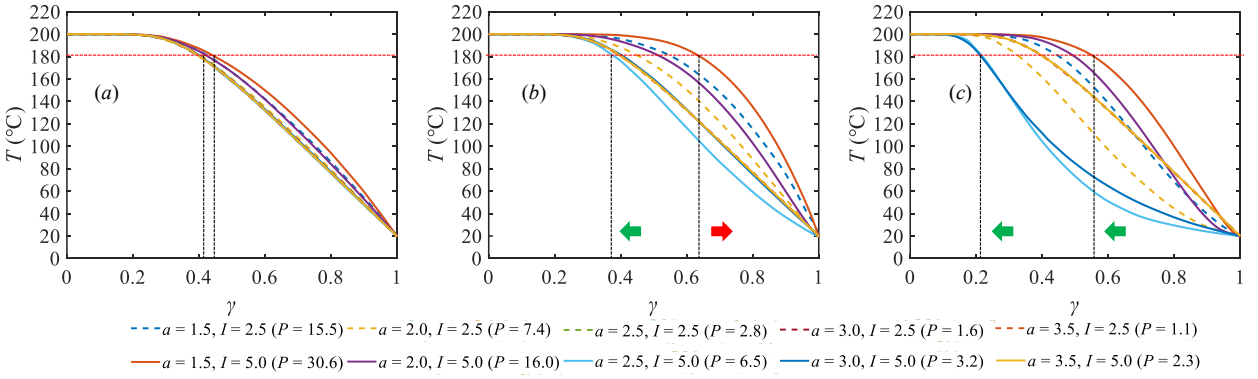

Figure 7 the evolutions of $T \sim I$. (*a*) p_{in} = 77.48MPa; (*b*) p_{in} = 75.10 MPa; (*c*) p_{in} = 76.00 MPa.

In order to minimize the effect of fracture stochastic generation, ten realizations are repeated for each combination of a and I and Table 2 gives the percentage of connected fracture networks in the ten realizations. Figure 8 depicts the variation of $\gamma_{(T = 180℃)}$ as a function of the percolation parameter in disconnected and connected DFNs, respectively. In overall tendency, if fracture networks are connected, $\gamma_{(T = 180℃)}$ firstly rises and then drops with the increasing of injection pressure. However, the larger percolation parameter P would have a higher extreme point and better capacity of heat production. Therefore, the observation of interactively superimposed geometrical and hydraulic effects indicates the high fracture intensity and connectivity can lead to high thermal sweep and heat extraction efficiency. Conversely, rocks with poor connectivity have small control areas of flow channeling which induces the rapid breakthrough of cold fluid under high pressure gradients. In addition, when p_{in} = 76.00 MPa, it can be noticed that $\gamma_{(T = 180℃)}$ at P = 15.5 decreases significantly compared with that at P = 16.0 although these two DFNs have similar permeability. It is speculated

that the smaller fracture length at the high fracture intensity (i.e. $I = 5.0$ m^{-1}) conduces to construct tortuous flow channels eventually leading to a higher heat extraction efficiency.

Table 2 the percentage of connected fracture networks in the ten realizations

I	*a*	*P*	Percentage (%)
2.5	1.5	15.5	100
	2.0	7.4	100
	2.5	2.8	0
	3.0	1.6	0
	3.5	1.1	0
5.0	1.5	30.6	100
	2.0	16.0	100
	2.5	6.5	50
	3.0	3.2	10
	3.5	2.3	0

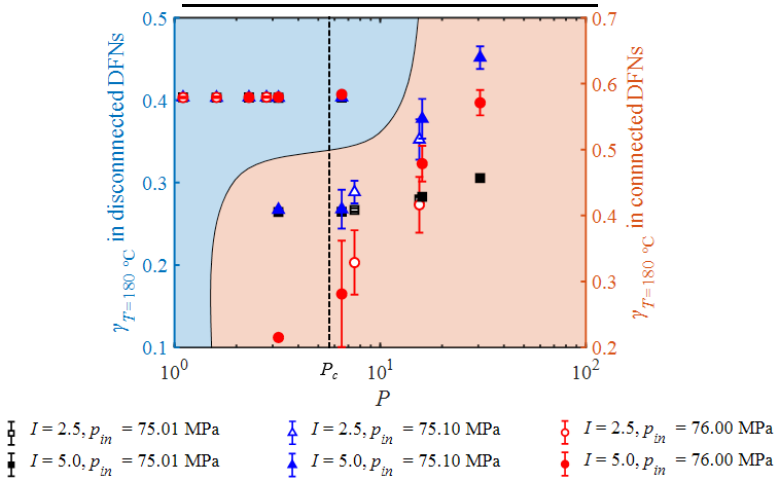

Figure 8 the variation of $\gamma_{(T=180^\circ C)}$ as a function of the percolation parameter *P* in disconnected and connected DFNs, respectively.

4. CONCLUSIONS

In this paper, a series of THM coupled governing equations are formulated as the mathematical model for the CO_2-EGS heat transfer process. A power-law model is used to describe the geometrical distribution of DFNs and three different pressure gradients are considered. The results can be concluded as follows:

- The effective permeability of reservoir plays a critical role in geothermal development. With the increasing mining time, the effective permeability increases until to a certain value, which means the system heat is exhausted. For the critical period of geothermal development, the initial permeability (or percolation parameter) has a significant contribution to heat production.

- It is found that both fracture distribution and hydraulic scenario generate important impact on heat extraction efficiency. With the increasing of pressure gradient, the heat recovery at the production temperature equal to 180°C firstly increases and then decreases. However, DFNs with a larger percolation parameter *P* would have a higher extreme point and better capacity of heat production.

- In order to attain higher thermal power in CO_2-EGS, the dense and interconnected fracture network is the crucial precondition. If the reservoir has a poor connectivity, the high production rate would not be profitable as it can cause the rapid breakthrough of cold fluid.

ACKNOWLEDGEMENTS

This study was jointly supported by the National Natural Science Foundation of China (Grant NO.51774317, Grant NO.51722406 and Grant NO. 61573018), the Fundamental Research Funds for the Central Universities (Grant No.18CX02100A) and Evaluation and Detection Technology Laboratory of marine mineral resources, Qingdao National Laboratory for Marine Science and Technology (Grant No. KC201702) and National Science and Technology Major Project (Grant NO.2016ZX05011004-004).

REFERENCES

Baria, R., Baumgärtner, J., Rummel, F., Pine, R.J., and Sato, Y.: Hdr/hwr reservoirs: concepts, understanding and creation. *Geothermics*, **28**, (1999), 533-552.

Bonnet, E., Bour, O., Odling, N. E., Davy, P., Main, I., Cowie, P., et al.: Scaling of fracture systems in geological media. *Reviews of Geophysics*, **39**, (2001), 347.

Bour, O., and Davy, P.: Connectivity of random fault networks following a power law fault length distribution. *Water Resources Research*, **33**, (1997), 1567-1584.

Cui, G.D., Zhang, L., Ren, B., Enechukwu, C., Liu, Y.M., Ren, S.R.: Geothermal exploitation from depleted high temperature gas reservoirs via recycling supercritical CO_2: Heat mining rate and salt precipitation effects. *Applied Energy*, **183**, (2016), 837-52.

Gisladottir, V.R., Roubinet, D., Tartakovsky, D.M.: Particle Methods for Heat Transfer in Fractured Media. *Transport in Porous Media*, **115**, (2016), 1-16.

Izadi, G., and Elsworth, D.: The influence of thermal-hydraulic-mechanical- and chemical effects on the evolution of permeability, seismicity and heat production in geothermal reservoirs. *Geothermics*, **53**, (2015), 385-395.

Jiang, F.M., Luo, L., and Chen, J.L.: A novel three-dimensional transient model for subsurface heat exchange in enhanced geothermal systems. *International Communications in Heat and Mass Transfer*, **41**, (2013), 57-62.

Li, J.W., Li, Z, Yuan, W.J., Lei, X.M., Sergio A.G.T, Claudia C, et al.: Numerical investigation of liquid and supercritical CO_2 flow behaviors through 3D self-affine rough fractures, *Fuel*, **251**, (2019), 669-682.

Mcdermott, C.I., Randriamanjatosoa, A. R. L., Tenzer, H., and Kolditz, O.: Simulation of heat extraction from crystalline rocks: The influence of coupled processes on differential reservoir cooling. *Geothermics*, **35**, (2006), 321-344.

Miller, S.A.: Modeling enhanced geothermal systems and the essential nature of large-scale changes in permeability at the onset of slip, *Crustal Permeability*, John Wiley & Sons, Ltd, (2016).

Nordqvist, A.W., Tsang, Y.W., Tsang, C.F., Björn, D., and Andersson, J.: A variable aperture fracture network model for flow and transport in fractured rocks. *Water Resources Research*, **28**, (1992), 1703-1713.

Pruess, K.: Enhanced geothermal systems (EGS) using CO_2 as working fluid—A novel approach for generating renewable energy with simultaneous sequestration of carbon. *Geothermics*, **35**, (2006), 351-367.

Sun, Z.X., Zhang, X., Xu, Y., Yao, J., Wang, H.X., Lv, S.H. et al.: Numerical simulation of the heat extraction in EGS with thermal-hydraulic-mechanical coupling method based on discrete fractures model. *Energy*, **120**, (2017), 20-33.

Xu, C.S., Dowd, P. A., and Tian, Z. F.: A simplified coupled hydro-thermal model for enhanced geothermal systems. *Applied Energy*, **140,** (2015), 135-145.

Yao, J., Zhang, X., Sun, Z.X., Huang, Z.Q., Liu, J.R., and Li, Y., et al.: Numerical simulation of the heat extraction in 3D-EGS with thermal-hydraulic-mechanical coupling method based on discrete fractures model. *Geothermics*, **74**, (2018), 19-34.

Zhao, Y.S., Feng, Z.J., Feng, Z.C., Yang, D., and Liang, W.G.: THM (Thermo-hydro-mechanical) coupled mathematical model of fractured media and numerical simulation of a 3D enhanced geothermal system at 573 K and buried depth 6000–7000 M. *Energy*, **82**, (2015), 193-205.